Nuclear Science and Techniques **22** (2011) 47–54

Structures and potential energy functions for ground states of PuU and U_2 molecules

LI Rusong* HE Bin ZHANG Quanhu

Xi'an Research Institute of Hi-Tech, Hongqing Town, Xi'an 710025, China

Abstract Pu-Pu, Pu-U and U-U interatomic potentials must be known in molecular dynamics (MD) calculation of the effects of U recoil nucleus produced by self irradiation on physical properties and phase stability in δ-Pu. Because of the lack of experimental data for fitting Pu-U and U-U potentials, electronic states and potential data of PuU and U_2 molecules are obtained by *ab initio* calculations with B3LYP hybrid exchange-correlation functional. The valence electrons of Pu and U atoms are treated with contraction basis sets, and the cores are approximated with relativistic effective core potential. The results show that electronic states for the ground states are $X^{11}\Sigma_u^+$ and $X^9\Sigma_g^+$. The pair potential data are fitted with the Murrell-Sorbie analytical potential function. The LDA+*U* calculations on the Pu-U intermetallic compound are performed with Perdew and Wang exchange-correlation functional at the spin-polarized level. The material parameters, such as the cohesive energies, elastic constants, and bulk modulus, are used to fit the 0-K universal Rose EOS, so the Pu-U EAM potential model is obtained.

Key words Ab initio, Electronic state, Dissociation energy, Potential

1 Introduction

Plutonium metallurgy lies at the heart of the scientific challenges to the nuclear stockpile. Aging mechanisms based on the atomic level are essential to assess the security and reliability of the weapon grade (WG) Pu materials. However, Pu element has six equilibrium solid and liquid phases at ambient pressure. Pu crystalline exists in the monoclinic α phase at room temperature, while it can be metastabilized in the fcc structure δ phase at room temperature by spiking certain elements, such as Al, Ga, or Am[1]. δ-Pu has been used as nuclear explosives since the Manhattan Project[2]. The ^{239}Pu nucleus releases helium particle of about 5 MeV and 86 keV U recoil nucleus. A He particle dissipates nearly 99.9% of its energy through collisions with electrons, and leads to thermal vibration of the Pu lattice. A recoil U nucleus would displace the Pu atoms, cause primary damage in the Pu lattice, and form the self-interstitial atom (SIA) and vacancy (Frenkel pair). About 2500 Frenkel pairs are generated in one decay event[3-5]. Although most Frenkel pairs would return to their original lattice sites in 200 ns, the residual Frenkel pairs form defects, such as vacancy, SIA or their clusters[6-8], which would cause lattice damage. Helium particles would lead to He bubble growth and latent void expansion, with corresponding macroscopic effects of density decrease, dimension expansion and creeping[9,10].

It is currently impossible to observe the aging mechanism in atomic level for ^{239}Pu, and it is radioactive and toxic. Then, computer simulation is an alternative approach. Some authors focus on the displacement cascade evolution of the U recoil nucleus, the point defects (vacancy, SIA and their clusters) properties and configurations, He-vacancy cluster and three-dimensional He bubble[11-15], but little attention is paid on effect of the U recoil nucleus on the physical properties (such as swelling and lattice parameters) and phase stability.

Because pseudopotential and theoretical potential based on density functional theory (DFT) are

---

Supported by Defence Project under Contract Number E/FJF007

* Corresponding author. *E-mail address*: rusong231@126.com

Received date: 2010-10-15

adequate for small system comprised of at most 1000 atoms. In this paper, atomic scale simulation for larger systems is performed with semiempirical or empirical potential. The parameters of interatomic potential are determined by fitting the *ab initio* calculation data or/and the experimental results (such as cohesive energy, lattice constants, bulk modulus and elastic constants). Due to lack of experiment data for PuU alloy, *ab initio* calculation of Pu-U and U-U pair potentials is performed. Analytic potential functions and electronic states for ground states are obtained. The analytic potential functions are then used as input data for molecular dynamics (MD) simulations of the U recoil nucleus effects.

2 Theoretical

For actinide elements of Pu and U, narrower 5*f* bands along with properties intermediate between those of localized 4*f* and delocalized 3*d* orbitals, near the Fermi level, are believed to be responsible for the exotic structure of actinides at ambient condition[16]. For light actinides with delocalized 5*f* electrons, the behavior is well described with standard DFT. However, for heavy actinides with localized 5*f* electrons, due to strong electron-electron interaction, conventional DFT fails to capture the localization effect of 5*f* electrons. Pu lies at the boundary between the light and heavy actinides, so it exhibits abnormal behaviors[17]. At the present time, the suitable methods are the hybrid exchange-correlation functional (such as B3LYP), the self-interaction correction (SIC), the dynamics mean field theory (DMFT), and the local density approximation (LDA) or the generalized gradient approximation (GGA)+*U*. The Hubbard *U* parameter represents a correction to the Coulomb repulsion interaction, separating the *f* manifold into lower and upper Hubbard bands and removing *f* degrees of freedom from the Fermi level[18-20].

Söderlind P, *et al*[21] observed that inclusions of spin-orbit coupling (SOC) are not essential for the quantitative behavior of δ-Pu. SOC affects equilibrium volume to a small extent and makes little energy changes between phases or elastic properties[22]. So the SOC effect is omitted in this paper.

In MD calculation of the effects of U recoil nucleus produced by self irradiation on the physical properties and phase stability in δ-Pu, Pu-Pu, U-U and Pu-U interatomic potentials must be known. Modified embedded atom method (MEAM) potential[23-25] can be used to describe Pu-Pu potential. Pu-U and U-U potentials can be determined from embedded atom method (EAM). The total energy E of atomic system in EAM (MEAM) formula is approximated as the sum of the embedding energy and the pair potential terms[26] in Eq.(1)

$$E = \sum_{i=1} \left(F_i(\bar{\rho}_i) + \frac{1}{2}\sum_{i\neq j} \varphi_{ij}(r_{ij})\right) \tag{1}$$

where the embedding function F is the energy to embed an atom of type i into the background electron density $\bar{\rho}_i$ at site i, and φ is the pair interaction between atoms i and j whose separation is given by R_{ij}.

The embedding energy is given by

$$F_i(\bar{\rho}_i) = A_i E_i^0 \ln(\bar{\rho}_i) \tag{2}$$

where the sublimation energy E_i^0 and parameter A_i depend on the element type of atom i. The background electron density $\bar{\rho}_i$ is given in Eq.(3) or Eq.(4)

$$\bar{\rho}_i = \frac{\rho_i^{(0)}}{\rho_i^0} \frac{2}{1+\exp(-\Gamma_i)} \tag{3}$$

$$\bar{\rho}_i = \frac{\rho_i^{(0)}}{\rho_i^0} (1+\Gamma_i)^{1/2} \tag{4}$$

where

$$\Gamma_i = \sum_{k=1}^{3} t_i^{(k)} \left(\frac{\rho_i^{(k)}}{\rho_i^{(0)}}\right)^2 \tag{5}$$

The partial electron densities $\rho_i^{(k)}$ (k=0, 1, 2, 3) are obtained from Eqs.(6a)–(6d)

$$\rho_i^{(0)} = \sum_{i\neq j} \rho_j^{a(0)}(r_{ij}) S_{ij} \tag{6a}$$

$$(\rho_i^{(1)})^2 = \sum_{\alpha} \left[\sum_{i\neq j} \rho_j^{a(1)} \frac{r_{ij\alpha}}{r_{ij}} S_{ij}\right]^2 \tag{6b}$$

$$(\rho_i^{(2)})^2 = \sum_{\alpha,\beta} \left[\sum_{i\neq j} \rho_j^{a(2)} \frac{r_{ij\alpha} r_{ij\beta}}{r_{ij}^2} S_{ij}\right]^2 - \frac{1}{3}\left[\sum_{i\neq j} \rho_j^{a(2)}(r_{ij}) S_{ij}\right]^2 \tag{6c}$$

$$(\rho_i^{(3)})^2=\sum_{\alpha,\beta,\gamma}\left[\sum_{i\neq j}\rho_j^{a(3)}\frac{r_{ij\alpha}r_{ij\beta}r_{ij\gamma}}{r_{ij}^3}S_{ij}\right]^2- \\ \frac{3}{5}\sum_{\alpha}\left[\sum_{i\neq j}\rho_j^{a(3)}\frac{r_{ij\alpha}}{r_{ij}}S_{ij}\right]^2 \tag{6d}$$

where $r_{ij\alpha}$, $r_{ij\beta}$ and $r_{ij\gamma}$ are the α, β and γ components of the displacement vector from atom i to atom j, S_{ij} is the screening function between atoms i and j. The screening of atoms i and j by an atom k is defined using an ellipse passing through the three atoms[24,26].

$$S_{ij}=\prod_{k\neq i,j}S_{ijk} \tag{7}$$

The equation of the ellipse is given by

$$x^2+\frac{y^2}{C}=(\frac{R_{ij}}{2})^2 \tag{8}$$

where

$$C=\frac{2(X_{ik}+X_{jk})-(X_{ik}-X_{jk})^2-1}{1-(X_{ik}-X_{jk})^2} \tag{9}$$

$$X_{ik}=\left(\frac{R_{ik}}{R_{ij}}\right)^2 \quad X_{jk}=\left(\frac{R_{jk}}{R_{ij}}\right)^2 \tag{10}$$

The screening factor S_{ijk} is determined as a function of C as follows:

$$S_{ijk}=f_c[(C-C_{\min})/(C_{\max}-C_{\min})] \tag{11}$$

where $C_{\min}$ and $C_{\max}$ are the limiting values of screening, the nominal values are $C_{\min}=1.4$ and $C_{\max}=2.8$. The smooth cutoff function $f_c(x)$ is given by

$$f_c(x)=\begin{cases}1 & x\geq 1\\ [1-(1-x)^4]^2 & 0<x<1\\ 0 & x\leq 0\end{cases} \tag{12}$$

During the modeling of Pu-U EAM potential, the value of the energy per atom for the equilibrium reference structure is obtained from the 0K universal equation of state (EOS) of Rose J H *et al*[27] as a function of the nearest-neighbor distance

$$F(\bar{\rho}^0(R)]+\frac{1}{2}\sum\Phi(R)=E^u(R) \\ =-E_c(1+a^*+\delta a^{*3})e^{-a^*} \tag{13}$$

$$a^*=\alpha(R/r_e-1) \tag{14}$$

$$\alpha=(9B\Omega/E_c)^{1/2} \tag{15}$$

where $E^u(R)$ is the universal function for a uniform expansion or contraction in the reference structure, r_e is the equilibrium nearest neighbor distance, B is the bulk modulus, and Ω is the equilibrium atomic volume, and δ is a parameter related to the pressure derivative of the bulk modulus of the reference phase.

If only first nearest-neighbor interactions are considered in the EAM, the total energy per atom can be given by

$$E^u(R)=F[\bar{\rho}^0(R)]+(Z_1/2)\Phi(R) \tag{16}$$

where Z_1 is the number of nearest-neighbor atoms. The expressions for the pair potential $\Phi(R)$ and the total energy per atom $E^u(R)$ are obtained from Eqs.(18) and (13), respectively. Because the local environment for individual Pu or U atom is similar, the expression for the embedding energy between two atoms separated by a distance R is obtained from Eq.(16) as follows:

$$F[\bar{\rho}^0(R)]=E^u(R)-(Z_1/2)\Phi(R) \tag{17}$$

For Pu-U and U-U pair potentials, potential data can be obtained from *ab initio* calculation. According to the atomic and molecular reaction statics (AMRS)[28], Pu atom and U atom belong to group SO(3). The irreducible representations of the electronic states for the ground states of Pu atom and U atom are $^7\mathrm{F_g}$ and $^5\mathrm{L_u}$, and they can be resolved into those of PuU/$\mathrm{U_2}$ ($\mathrm{C_{\infty V}/D_{\infty h}}$), these procedures can be given by

Pu: $^7\mathrm{F_g}\rightarrow{}^7\Sigma_\mathrm{g}^-\oplus{}^7\mathrm{II_g}\oplus{}^7\Delta_\mathrm{g}\oplus{}^7\Phi_\mathrm{g}$

U: $^5\mathrm{L_u}\rightarrow{}^5\Sigma_\mathrm{u}^-\oplus{}^5\mathrm{II_u}\oplus{}^5\Delta_\mathrm{u}\oplus{}^5\Phi_\mathrm{u}\oplus{}^5\Gamma_\mathrm{u}\oplus\ldots$

So the possible electronic states for PuU molecule are

$^7\mathrm{F_g}\otimes{}^5\mathrm{L_u}=({}^7\Sigma_\mathrm{g}^-\oplus{}^7\mathrm{II_g}\oplus{}^7\Delta_\mathrm{g}\oplus{}^7\Phi_\mathrm{g})\otimes({}^5\Sigma_\mathrm{u}^-\oplus{}^5\mathrm{II_u}\oplus{}^5\Delta_\mathrm{u}\oplus{}^5\Phi_\mathrm{u}\oplus{}^5\Gamma_\mathrm{u}\oplus\ldots)={}^{3,5,7,9,11}\Sigma_\mathrm{u}^+(4)\oplus{}^{3,5,7,9,11}\mathrm{II_u}(6)\oplus{}^{3,5,7,9,11}\Delta_\mathrm{u}(5)\oplus{}^{3,5,7,9,11}\Phi_\mathrm{u}(4)\oplus{}^{3,5,7,9,11}\Gamma_\mathrm{u}(3)\oplus{}^{3,5,7,9,11}[\Sigma_\mathrm{u}^-](3)\oplus{}^{3,5,7,9,11}\mathrm{H_u}(2)\oplus{}^{3,5,7,9,11}\mathrm{I_u}\oplus\ldots$

Similarly, the possible electronic states for $\mathrm{U_2}$ molecule are $^{1,3,5,7,9}\Sigma_\mathrm{g}^+(5)$, $^{1,3,5,7,9}\mathrm{II_g}(6)$, $^{1,3,5,7,9}\Delta_\mathrm{g}(5)$, $^{1,3,5,7,9}\Phi_\mathrm{g}(5)$, $^{1,3,5,7,9}\Gamma_\mathrm{g}(5)$, $^{1,3,5,7,9}[\Sigma_\mathrm{g}^-](3)$, $^{1,3,5,7,9}\mathrm{H_g}(2)$ and $^{1,3,5,7,9}\mathrm{I_g}(2)\ldots$

In the *ab initio* calculations for Pu-U and U-U pair potentials, the valence electrons of Pu atom can be treated with (7*s*6*p*2*d*4*f*)/[3*s*3*p*2*d*2*f*] contraction basis set, and the core is approximated with relativistic effective core potential (RECP). Similarly, the valence electrons of U atom can be treated with (5*s*4*p*3*d*4*f*) / [3*s*3*p*2*d*2*f*] contraction basis set, and the core is also approximated with RECP. The Pu-U and U-U pair potential data are predicted with Becke-3 hybrid exchange-correlation functional (B3LYP) with the Gaussian09w code[29-32], and they can be fitted with the modified Murrell-Sorbie analytical potential function. The convergence of self-consistent field (SCF) is less than 1×10^{-8}.

$$\Phi = D_e(1+\sum_{l=1}^{n} a_l d^l)\exp(a_l d) \tag{18}$$

where D_e is the dissociation energy, $d = r - r_e$, r is interatomic distance, r_e is interatomic equilibrium distance, and a_l and n are potential function parameters.

The LDA+*U* calculations on Pu-U intermetallic compound ($L1_2$ structure) have been performed using Perdew and Wang (PW) exchange-correlation functional at the spin-polarized (SP) level within the plane augmented wave (PAW) method as implemented in the ABINIT code[33]. This package is based on an efficient fast Fourier transform algorithm for the conversion of wave functions between real and reciprocal space, on the adaptation to a fixed potential of the band-by-band conjugate-gradient method[34] and on a potential-based conjugate-gradient algorithm for determining the self-consistent potential.

The LDA+*U* (Hubbard *U* parameter separating the *f* manifold into lower and upper Hubbard bands and removing *f* degrees of freedom from the Fermi level) method is designed by combining DFT+LDA and a Hubbard-type term in the Hamiltonian. The contribution to energy is the sum of the LDA energy for a given density, the electron-electron interaction term E_{ee} from the Hubbard term and a double counting term, $E_{LDA+U}[n_{LDA+U}]=E_{LDA}[n_{LDA+U}]+E_{ee}-E_{dc}$. The last two terms are functions of the occupation matrix $n^{\sigma}_{1,2}$ in a given basis[18].

A plane-wave cutoff energy E_{cut}=400 eV is chosen for Pu-U intermetallic compound. The calculations are performed by a 10×10×10 Monkhorst-Pack grid and the improved tetrahedron method with Gaussian smearing (0.1 eV). The cores of Pu atom and U atom are approximated with ultra-soft pseudopotential (USPP). The convergence of self-consistent field (SCF) is $<1.0\times10^{-5}$ eV/atom. For the exchange-correlation energy, the Perdew-Wang (PW) functional is used for LDA. U=4.0 eV and J=0.7 eV are employed for the Hubbard *U* parameter[35].

For the Pu_mU_n stoichiometric compound, assuming the homogeneous interatomic interaction is the same as the interaction in the pure material, the cohesive energy can be given by

$$E_c = \frac{m}{m+n}E_c^{Pu} + \frac{n}{m+n}E_c^{U} + \Delta H_f \tag{19}$$

where E_c^{Pu} and E_c^{U} are the cohesive energies of pure δ phase Pu and γ phase U, respectively.

$$\Delta H_f = \frac{E_{tot} - m\varepsilon_{Pu} - n\varepsilon_U}{m+n} \tag{20}$$

where ΔH_f is formation enthalpy per atom, E_{tot} is the total energy of the system, *m* and *n* are the numbers of Pu and U atoms in the system, and ε_{Pu} and ε_U are the total energies per atom for Pu atom and U atom in the reference structures (*δ* phase fcc structure and *γ* phase bcc structure, respectively).

3 Results and discussion

3.1 Structure and potential function of PuU

As described above, the multiplicities of PuU are 3, 5, 7, 9 and 11, respectively. And the unpaired electrons are 2, 4, 6, 8 and 10, respectively. Because of the multiple effects of configuration mixture and hybrid of Pu 5*f* electrons with U 5*f* electrons, several minimum potentials appear in Pu-U pair potential (Table 1).

When the multiplicity of PuU is 11, and Pu-U interatomic distance is 0.44 nm, PuU molecule is the most stable, so the electronic state for the ground state is $X^{11}\Sigma_u^+$. Then the Murrell-Sorbie analytical potential function is used to fit the potential data with regular equations, the fitting result is shown in Table 2. *Ab initio* calculation data is compared with Murrell-Sorbie fitting results in Fig.1.

Table 1 *Ab initio* calculation data of PuU multiplicity. $E_{\min}$ is the minimum potential and $R_{\min}$ is Pu-U interatomic distance

Multiplicity	$R_{\min}$ /nm	$E_{\min}$/a.u.	$R_{\min}$ /nm	$E_{\min}$/a.u.	$R_{\min}$ /nm	$E_{\min}$/a.u.	$R_{\min}$ /nm	$E_{\min}$/a.u.	$R_{\min}$ /nm	$E_{\min}$/a.u.
3	0.30	–123.0200	0.44	–123.1601	—	—	—	—	—	—
5	0.325	–123.1113	—	—	—	—	—	—	—	—
7	0.34	–123.1489	0.37	–123.1495	0.39	–123.1492	0.41	–123.1505	0.45	–123.2117
9	0.34	–123.2043	0.39	–123.2355	—	—	—	—	—	—
11	0.35	–123.2190	0.44	–123.2773	—	—	—	—	—	—

Table 2 Disassociation energies and the parameters of the Murrell-Sorbie analytical potential functions for the electronic state $X^{11}\Sigma_u^+$ of PuU and the electronic state $X^9\Sigma_g^+$ of U_2 molecule

Molecules	D_e(eV)	a_1(nm^{-1})	a_2(nm^{-2})	a_3(nm^{-3})	a_4(nm^{-4})	a_5(nm^{-5})	a_6(nm^{-6})
PuU	1.4278	5.527	–94.2	209.8	–217.5	—	—
U_2	0.5656	7.177	–243.1	93.89	–2377	5027	–7366

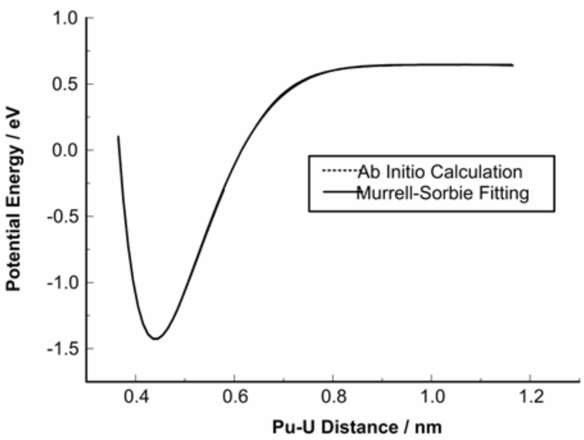

Fig.1 Comparison of *ab initio* and Murrell-Sorbie fitting potentials as a function of Pu-U interatomic distance.

3.2 Structure and potential function of U_2

Similarly, the multiplicities of U_2 are 1, 3, 5, 7 and 9, the unpaired electrons are 0, 2, 4, 6 and 8, respectively. Because of U 5*f* electrons hybrid with 6*d* electrons and the configuration mixture effect, the outer-shell orbits may be the multiple contributions from 5*f* electrons, 7*s* electrons and other electrons. The electronic states are undetermined. With an initial guess of orbital changes in the calculation, we predict several minimum potentials, as shown in Table 3.

When the multiplicity of U_2 molecule is 9, and U-U interatomic distance is 0.33 nm, U_2 molecule is the most stable, so the electronic state for the ground state is $X^9\Sigma_g^+$. Then the Murrell-Sorbie analytical potential function is used to fit the potential data with regular equations (Table 2). *Ab initio* calculation data is compared with Murrell-Sorbie fitting result in Fig.2.

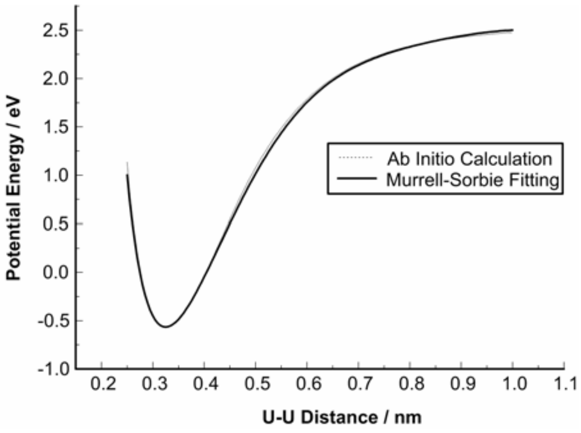

Fig.2 Comparison of *ab initio* and Murrell-Sorbie fitting potentials as a function of U-U interatomic distance.

Table 3 *Ab initio* calculation results of U_2 multiplicity. $E_{\min}$ is the minimum potential and $R_{\min}$ is U-U interatomic distance

Multiplicities	$R_{\min}$ /nm	$E_{\min}$ /a.u.	$R_{\min}$ /nm	$E_{\min}$ /a.u.	$R_{\min}$ /nm	$E_{\min}$ /a.u.
1	0.31	–102.6794	0.4	–102.7629	—	—
3	0.30	–102.7752	0.37	–102.8080	0.51	–102.8401
5	0.325	–102.9483	—	—	—	—
7	0.31	–102.8774	0.36	–102.9079	0.48	–102.9490
9	0.33	–102.9557	0.38	–102.9540	—	—

3.3 Calculation on Pu-U intermetallic compound

It is known that Pu lies at the boundary between the light actinides with delocalized 5*f* electrons and the heavy actinides with localized 5*f* electrons, so Pu *f* state is dynamical, and the *f* electrons may freely fluctuate between a localized f^4 shell and a fully itinerant state[36]. In this work, Pu 5*f* electrons are in f^5 configuration (four 5*f* electrons localized in an atomic singlet, leaving one itinerant 5*f* electron contributing to the chemical bond). Spin polarization is used to simulate the effect of *f*-electron localization, to predict a non-magnetic ground state of δ-Pu with both lattice parameter and bulk modulus in good agreement with experiment value.

However, spin polarization causes exchange splitting of 5*f*-orbitals, hence partial removal of 5*f* states from the Fermi level, and is apt to weaken 5*f* contribution to the chemical bonding and increase localization behavior and the equilibrium volume values, meanwhile, almost no *f* electrons in the vicinity of the Fermi level. This is similar to the work of Shorikov A O, *et al*[37] but in sharp contradiction to the experimental photoemission spectra (PES), where the high peak attributed to *f* states is clearly observed at the Fermi level[38]. A possible reason is that the local Coulomb interaction *U* promotes the splitting of 5*f* shell into the completely filled $f^{5/2}$ and empty $f^{7/2}$ states. Therefore, LDA+*U* calculations of δ phase Pu result in a nonmagnetic configuration with the filled $f^{5/2}$ and empty $f^{7/2}$ states.

In fact, The LDA+*U* approach corresponds to the static limit of a more general LDA+DMFT approach. Taking account of the dynamics terms of an energy (or time) dependent self-energy, the dynamical mean-field theory (DMFT)[39] can not only reproduce the ground-state properties, such as volume and moments, but also provide the spectral density agreement with the experimental PES.

For U element, all *f* electrons are treated as itinerant (delocalized 5*f* electrons in f^3 configuration). The calculated electronic structure agrees with that in Ref.[40]. Large change in electron coupling behavior is due to the delocalized nature of the 5*f* states in U, rather than localized nature of the 5*f* states in Pu[41].

Fig.3 shows the calculated partial 5*f* states (spin up part) DOSs of U, Pu, and Pu-U compound. It can be seen that a visible Pu 5*f* peak appears at the Fermi level, indicating that Pu *f* states may hybrid with U *spdf* states. Because the dominant contribution to hybridization function may not be the *f*-*f* hybridization but the *f*-*spd* hybridization[42,43] instead, the chemical substitution of Pu by U may lead to the occurrence of a 5*f* peak at the Fermi level.

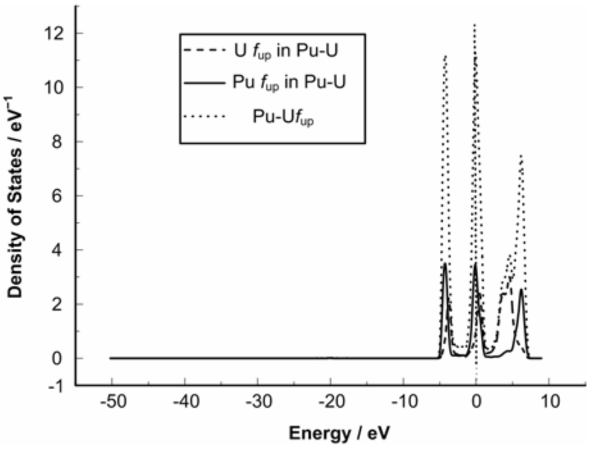

Fig.3 Partial 5*f* (spin up part) densities of states for U, Pu and Pu-U in Pu-U intermetallic compound ($L1_2$ structure) by LDA+*U* calculations. The Fermi level (dotted line) is at 0 eV.

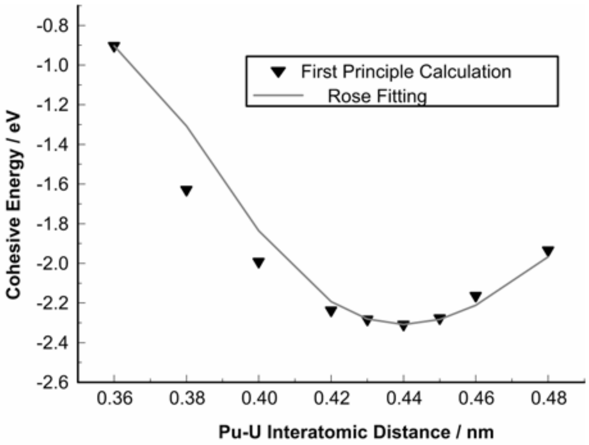

Fig.4 The calculated cohesive energy (▼) as a function of the interatomic distance for Pu-U intermetallic compound in $L1_2$ structure compared with the Rose fitting result (solid line).

For Pu-U intermetallic compound ($L1_2$ structure), the LDA+*U* results are given in Table 4. According to Eqs.(19) and (20), the cohesive energies as a function of Pu-U interatomic distance are obtained (Fig.4). The exponential decay factor α is evaluated with the bulk modulus B and the atomic volume Ω. In Table 4, E_c is the sublimation energy, the equilibrium interatomic distance is r_e, and δ is obtained from the fitting of cohesive energy with different interatomic distance to the 0K universal equation of state (EOS) of Rose J H *et al*[27].

Table 4 LDA+*U* results and EAM potential parameters for Pu-U intermetallic compound

Parameters	Values
C_{11}	131.4252
C_{12}	39.3867
C_{44}	64.3179
B	86.6870
E_c^{Pu} (δ phase Pu)	3.800
E_c^{U} (γ phase U)	6.8534
$E_c^{\mathrm{Pu\text{-}U}}$	2.3084
α (dimensionless)	6.7029
r_e	0.44
δ (dimensionless)	–0.1847

The elastic constants C_{11}, C_{12} and C_{44}, and the bulk modulus B, are in GPa. The sublimation energy E_c is in eV. The equilibrium interatomic distance r_e is in nm, respectively. The exponential decay factor for the universal Rose EOS α and the parameter related to the pressure derivative of the bulk modulus of the reference phase δ are given, too.

4 Conclusion

The electronic states and pair potential data of PuU and U_2 molecules are obtained by *ab initio* calculation with B3LYP hybrid exchange-correlation functional. The valence electrons of Pu and U atoms are treated with contraction basis sets, and the cores are approximated with RECP. The results show that the electronic states for the ground states are $X^{11}\Sigma_u^+$ and $X^9\Sigma_g^+$. The pair potential data are fitted with the Murrell-Sorbie analytical potential function. LDA+*U* calculations on the Pu-U intermetallic compound ($L1_2$ structure) are performed with PW exchange-correlation functional at the spin-polarized level, and physical properties of the cohesive energy, the equilibrium interatomic distance, the elastic constants, and the bulk modulus are evaluated. The data are fitted to the 0-K universal Rose EOS, so the Pu-U EAM potential model is obtained.

We are planning to construct the U-U EAM potential based on experimental data and the first principle calculations, so as to verify the reliability and flexibility under circumstances that have not been used during the construction phases. The potentials will be adopted to perform MD calculation of the effects of U recoil nucleus on physical properties of the volumetric expansion, the lattice parameters and elastic constants, and the phase stability in *δ*-Pu. The MD results with the migration energies, the formation energies and the mobilities of point defects can be used as the input data of the mesoscopic Monte Carlo (MMC) and the rate equations simulations.

Acknowledgements

The authors thank Dr. Li Wen for valuable discussions and support.

References

1 HECKER S S. Metall Mater Trans, 2008, **A39**: 1585–1592.

2 Baclet N, Oudot B, Grynszpan R, *et al.* J Alloys Compd, 2007, **444/445**: 305–309.

3 Chung B W, Thompson S R, Lema K E, *et al.* J Nucl Mater, 2009, **385:** 91–94.

4 Dremov V, Sapozhnikov P, Kutepov A. Phys Rev, 2008, **B77:** 224306.

5 Schwartz A J, Wall M A, Wolfer W G, *et al.* J Alloys Compd, 2007, **444/445**: 4–10.

6 Ao B Y, Wang X L, Hu W Y, *et al.* J Alloys Compd, 2007, **444/445:** 300–304.

7 Caturla M J, Soneda N, Fluss M, *et al.* J Nucl Mater, 2006, **351**: 78–87.

8 Caturla M J, Diaz de la Rubia T, Fluss M. J Nucl Mater, 2003, **323**: 163–168.

9 Chung B W, Thompson S R , Woods C H, *et al.* J Nucl Mater, 2006, **355:** 142–149.

10 Robinson M, Kenny S D, Smith R, *et al.* Nucl Instrum Meth**,** 2009, **B267:** 2967–2970.

11 Valone S M, Baskes M I, Stan M, *et al.* J Nucl Mater**,** 2004, **324:** 41–51.

12 Berlu L, Jomard G, Rosa G, *et al.* J Nucl Mater, 2008, **374:** 344–353.

13 Jomard G, Berlu L, Rosa G, *et al.* J Alloys Compd, 2007, **444/445:** 310–313.

14 Berlu L, Jomard G, Rosa G, *et al.* J Nucl Mater, 2008, **372:** 171–176.

15 Wheeler D W, Bayer P D. J Alloys Compd, 2007, **444/445:** 212–216.

16 Huda M N, Ray A K. Euro Phys, 2004, **B40:** 337–346.

17 Sun B, Zhang P, Zhao X G. J Chem Phys, 2008, **128:** 084705.

18 Jomard G, Amadon B, Bottin F. Phys Rev, 2008, **B78:** 075125.

19 Savrasov S Y, Kotliar G. Phys Rev Lett, 2000, **84:** 3670.

20 Shorikov A O, Lukoyanov A V, Korotin M A, *et al.* Phys Rev, 2005, **B72:** 024458.

21 Söderlind P, Landa A, Sadigh B. Phys Rev, 2002, **B66:** 205109.

22 Söderlind P, Sadigh B. Phys Rev Lett, 2004, **92:** 185702.

23 Daw M S, Baskes M I. Phys Rev Lett, 1983, **50:** 1285–1288.

24 Baskes M I. Phys Rev, 1992, **B46:** 2727–2742.

25 Baskes M I, Muralidharan K, Stan M, *et al.* JOM. 2003, **55:** 41–50.

26 Jelinek B, Houze J, Baskes M I, *et al.* Phys Rev, 2007, **B75:** 054106.

27 Rose J H, Smith J R, Guinea F, *et al.* Phys Rev, 1984, **B29:** 2963–2969.

28 Zhu Z H. Atomic and Molecular Reaction Statics. Beijing: Science Press, 2007, 56–62 (in Chinese).

29 Becke A D. J Chem Phys**,** 1993, **98:** 5648–5652.

30 Lee C, Yang W, Parr R G. Phys Rev B**,** 1988, **37:** 785–789.

31 Hay P J, Martin R L. J Chem Phys, 1998, **109:** 3875–3881.

32 Frisch M J, Trucks G W, Schlegel H B, *et al.* Gaussian 09 Package. Gaussian, Inc., Pittsburgh PA, 2009.

33 Jollet F, Jomard G, Amadon B. Phys Rev, 2009, **B80:** 235109.

34 Payne M C, Teter M P, Allan D C, *et al*. Rev Mod Phys, 1992, **64:** 1045–1097.

35 Shick A B, Drchal V, Havela L. Europhys Lett, 2005, **69:** 588–594.

36 Svane A, Petit L, Szotek Z, *et al*. Phys Rev, 2007, **B76:** 115116.

37 Shorikov A O, Lukoyanov A V, Korotin1 M A, *et al*. Phys Rev, 2005, **B72:** 024458.

38 Arko A J, Joyce J J, Morales L, *et al*. Phys Rev, 2000, **B62:** 1773.

39 Anisimov V I, Poteryaev A I, Korotin M A, *et al*. J Phys Condens Matter, 1997, **9**: 7359–7367.

40 Jones M D, Albers R C. Phys Rev, 2009, **B79:** 045107.

41 Moore K T, van der Laan G, Haire R G, *et al*. Phys Rev, 2006, **B73:** 033109.

42 Toropova A, Marianetti C A, Haule K, *et al*. Phys Rev, 2007, **B76:** 155126.

43 Shim J H, Haule K, Savrasov S. Phys Rev Lett, 2008, **101:** 126403.